

## Investigations of the transverse bulk polaritons in uniaxial Al<sub>2</sub>O<sub>3</sub> by infrared reflection

Y. T. Chu and J. B. Bates

*Solid State Division, Oak Ridge National Laboratory, Oak Ridge, Tennessee 37831*

(Received 25 November 1985)

The transverse bulk polariton dispersion curves in the region above 400 cm<sup>-1</sup> in uniaxial Al<sub>2</sub>O<sub>3</sub> were determined from the inflection points on the smooth edges of the high-reflectivity bands in infrared spectra measured at various angles of incidence for TM polarization.

### INTRODUCTION

Polaritons result from the strong coupling of an electromagnetic wave with an elementary excitation of a crystal. The elementary excitation may be a phonon, a plasmon, an exciton, a magnon, or a phonon-plasmon, etc. The existence of polaritons was first demonstrated experimentally by Henry and Hopfield<sup>1</sup> in GaP by means of forward and near-forward Raman scattering. Using the Raman scattering technique, one is able to trace out the polariton dispersion curves by varying the angle between the direction of incident beam and the direction of the scattered beam in the crystal.

Falge, Otto, and Sohler<sup>2</sup> and Nitsch, Falge, and Claus<sup>3</sup> proposed a simple straightforward method for measuring the dispersion of bulk polaritons by infrared reflection. This method is based on the fact that polaritons are already inherent in the solution of Maxwell's equations for a crystal characterized by its dielectric function. If one neglects damping in the expression of the dielectric function, the calculated spectrum exhibits high-reflectivity regions ( $R = 1$ ) bounded by steeply rising and falling edges. The frequencies corresponding to these edges depend on the values of the wave vector. Analysis shows that these edges are close to the frequencies of the polariton modes. Since the edges of the measured high-reflectivity bands ( $R < 1$ ) are smooth, we could define the inflection points on the boundaries as these edges. Thus the polariton dispersion curves could be traced out by measuring the inflection points obtained for various wave vectors which can be achieved by varying the angle of incidence or changing the index of refraction of the surrounding medium. This method has the advantage that it does not require analysis of experimental data.<sup>4-6</sup>

In this paper we report the dispersion of polaritons in uniaxial Al<sub>2</sub>O<sub>3</sub> single crystals measured by infrared reflection. The theoretical dispersion curves, calculated from the dielectric functions with damping neglected and from a response function derived by Barker and Loudon<sup>7</sup> with damping included, are compared with the experimental results.

### THEORY

We consider a TM polarized wave incident upon a uniaxial crystal. The orientation of the optic axis ( $c$  axis) is arranged to be parallel to one of the Cartesian coordinates, namely,  $\hat{c} \parallel \hat{y}$ ,  $\hat{c} \parallel \hat{z}$ , and  $\hat{c} \parallel \hat{x}$  (see Fig. 1). Hence the dielectric tensor for a uniaxial crystal is in diagonal form, and

the dielectric function is characterized by the principal values  $\epsilon_{\perp}$  and  $\epsilon_{\parallel}$ . The reflectivity  $R$  (Refs. 8 and 9) of these configurations can be derived from Maxwell's equations:

$$R(\theta, \omega) = \frac{\left| \frac{\epsilon_x^{1/2} \epsilon_z^{1/2} (\omega/c) \cos \theta - N_m [(\omega^2/c^2) \epsilon_z - k_x^2]^{1/2}}{\epsilon_x^{1/2} \epsilon_z^{1/2} (\omega/c) \cos \theta + N_m [(\omega^2/c^2) \epsilon_z - k_x^2]^{1/2}} \right|^2}{(1)}$$

where  $\theta$  is the incident angle,  $\omega$  is the angular frequency,  $c$  is the velocity of light in vacuum,  $N_m$  is the refractive index of the medium outside the crystal,  $\epsilon_x$  and  $\epsilon_z$  are the dielectric functions of the crystal, and  $k_x$  is the wave vector along the  $x$  direction. The latter is determined by

$$k_x = (\omega/c) N_m \sin \theta. \quad (2)$$

For the case of  $\hat{c} \parallel \hat{y}$ , one has  $\epsilon_x = \epsilon_z = \epsilon_{\perp}$  [see Fig. 1(a)]. Thus the crystal is equivalent to an optically isotropic crystal, and the reflectivity can be obtained from Eq. (1) simply by replacing  $\epsilon_x$  and  $\epsilon_z$  with  $\epsilon_{\perp}$ .

In order to simplify the analysis and preserve the essential features of the reflectivity, one may neglect damping in the expression of the dielectric functions.<sup>10</sup> The calculated  $\epsilon_{\perp}$  and  $\epsilon_{\parallel}$  with zero damping are plotted in Fig. 2. It can be seen that  $\epsilon_{\perp}$  and  $\epsilon_{\parallel}$  have negative values within the transverse (TO) and longitudinal (LO) optic mode frequencies and positive values outside these mode frequencies. Since there are four modes for  $\mathbf{E} \perp \hat{c}$  and two modes for  $\mathbf{E} \parallel \hat{c}$ , there are five bulk polariton dispersion curves for the cases  $\hat{c} \parallel \hat{y}$  and  $\hat{c} \parallel \hat{x}$  and three for the case  $\hat{c} \parallel \hat{z}$ . If one neglects damping, the factor  $(\omega/c) \sqrt{\epsilon_z}$  in Eq. (1) is just the wave vector  $k_B$  of the transverse bulk polaritons propagating along the  $x$  axis with the lattice displacements

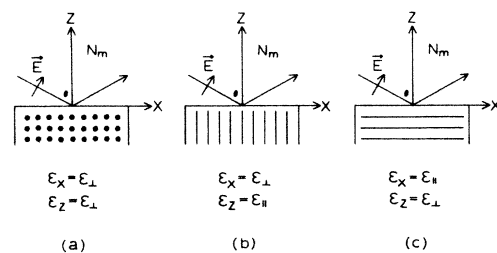


FIG. 1. Geometries for the experiment. The diagrams represent the orientations of the crystal for the three cases: (a)  $\hat{c} \parallel \hat{y}$ , (b)  $\hat{c} \parallel \hat{z}$ , (c)  $\hat{c} \parallel \hat{x}$ .

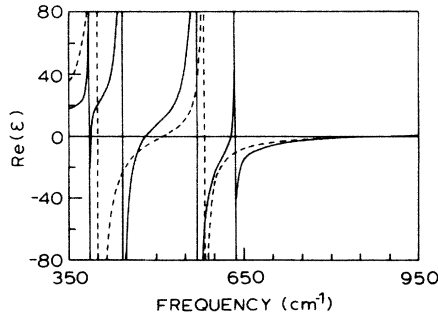


FIG. 2. The solid and dashed lines are, respectively, the dielectric function  $\epsilon_{\perp}$  and  $\epsilon_{\parallel}$  for  $\text{Al}_2\text{O}_3$  crystal calculated from Ref. 10 with damping neglected.

parallel to the  $z$  axis. Thus Eq. (1) can be transformed into

$$R(\theta, \omega) = \left| \frac{\epsilon_x^{1/2} k_B \cos\theta - N_m (k_B^2 - k_x^2)^{1/2}}{\epsilon_x^{1/2} k_B \cos\theta + N_m (k_B^2 - k_x^2)^{1/2}} \right|^2, \quad (3)$$

with

$$k_B = \frac{\omega}{c} \sqrt{\epsilon_z}. \quad (4)$$

From the above two equations, total reflection ( $R=1$ ) occurs when either one of the terms in the numerator of Eq. (3) is imaginary or equal to zero. Thus the regions of total reflection can be determined, if the following conditions are satisfied:

For  $\hat{c} \parallel \hat{y}$ ,

$$\text{I. } \epsilon_{\perp} \leq 0, \quad (5a)$$

$$\text{II. } \epsilon_{\perp} \geq 0, k_B^2 - k_x^2 \leq 0. \quad (5b)$$

For  $\hat{c} \parallel \hat{z}$  or  $\hat{c} \parallel \hat{x}$ ,

$$\text{I. } \epsilon_z \leq 0, \epsilon_x \leq 0, \quad (6a)$$

$$\text{II. } \epsilon_z \geq 0, \epsilon_x \leq 0, k_B^2 - k_x^2 \geq 0, \quad (6b)$$

$$\text{III. } \epsilon_z \geq 0, \epsilon_x \geq 0, k_B^2 - k_x^2 \leq 0. \quad (6c)$$

The frequencies corresponding to the edges of high-reflectivity regions determined from conditions (5a) and (6a) are the TO and LO mode frequencies, and they are independent of the incident angle. On the other hand, the frequencies corresponding to those edges determined from conditions (5b), (6b), and (6c) with  $k_B^2 - k_x^2 = 0$  are the polariton mode frequencies, and these frequencies depend on the incident angle and refractive index of the surrounding medium.

#### EXPERIMENTAL RESULTS AND DISCUSSION

Optically flat  $\text{Al}_2\text{O}_3$  crystals were cut into parallelepipeds measuring  $1 \times 1 \times 0.3 \text{ cm}^3$  with the  $c$  axis parallel or normal to the large faces. In order to obtain values of  $k_x$  greater than  $\omega/c$ , an equilateral KRS-5 prism (apex angle =  $120^\circ$ ) with index of refraction  $N_m = 2.35$  was used in the experiment which permitted reflectivity spectra to be obtained at angles of incidence  $\theta$  from  $26^\circ$  to  $34^\circ$ . The incident wave was polarized in the plane of incidence by a

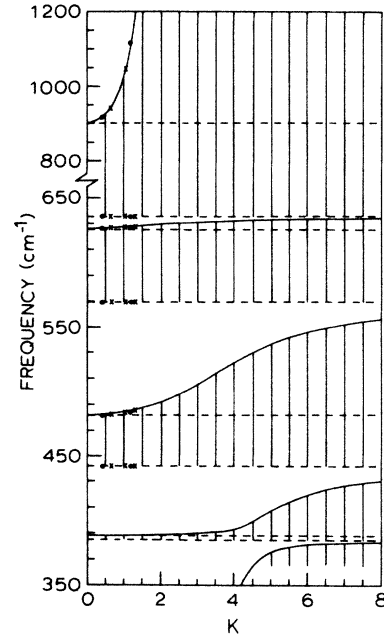


FIG. 3. Bulk polariton dispersion curves of  $\text{Al}_2\text{O}_3$  (solid lines) for the case  $\hat{c} \parallel \hat{y}$ . See text for detail.

metal wire grid polarizer on a KRS-5 substrate. All experiments were performed at room temperature with a resolution of  $2 \text{ cm}^{-1}$  using a Digilab model No. FTS-20 Fourier-transform spectrometer, and the spectra were recorded in the region above  $400 \text{ cm}^{-1}$ . The polariton dispersion curves in the region below  $400 \text{ cm}^{-1}$  cannot be determined in our experiment, since correspondingly large wave vectors were not accessible. Therefore, only three polariton dispersion curves for  $\hat{c} \parallel \hat{y}$  and  $\hat{c} \parallel \hat{x}$  ( $\epsilon_z = \epsilon_{\perp}$ ) and two polariton dispersion curves for  $\hat{c} \parallel \hat{z}$  ( $\epsilon_z = \epsilon_{\parallel}$ ) were determined in our experiment.

In Figs. 3, 5, and 7, the solid lines are the calculated polariton dispersion curves from Eq. (4) with zero damping, and the dashed lines are the TO and LO mode frequencies. The hatched areas are the high-reflectivity regions determined from conditions (5a) and (5b) for Fig. 3, and from conditions (6a)–(6c) for Figs. 5 and 7. The closed circles and crosses are the measured results. Note that a dimensionless quantity  $K$  is defined as  $(c/\omega)k_B$  or  $(c/\omega)k_x$

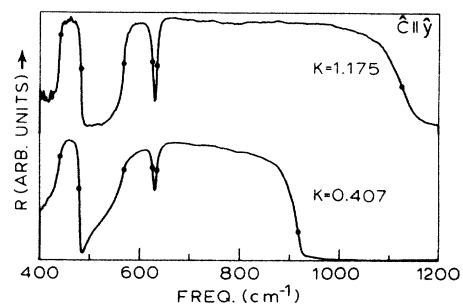
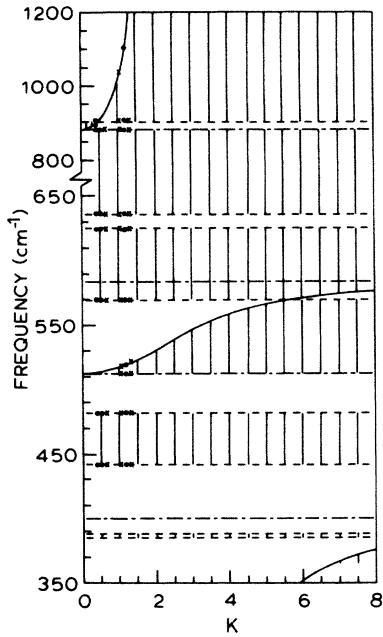
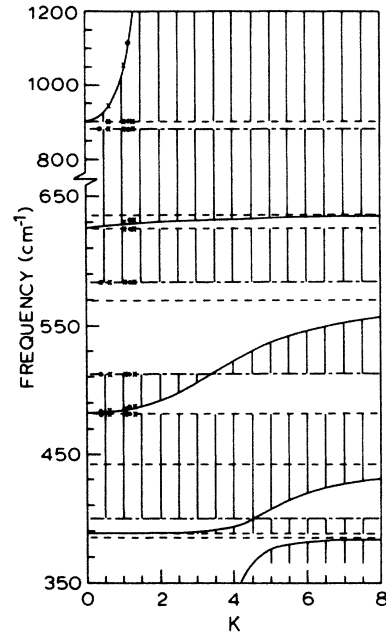


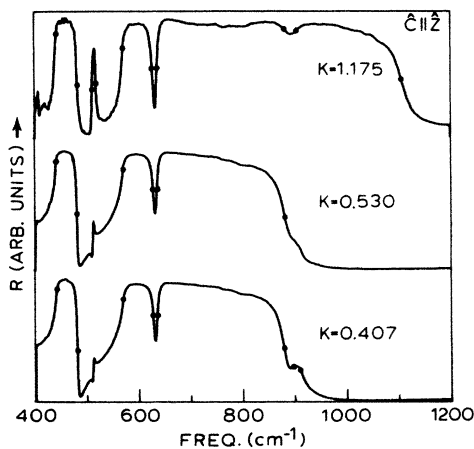
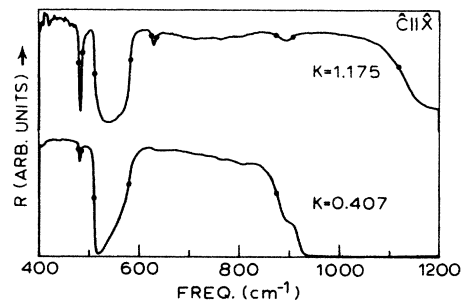
FIG. 4. Measured reflectivity spectra for the case  $\hat{c} \parallel \hat{y}$ . The closed circles are the inflection points on the edges of the high-reflectivity bands.

FIG. 5. The same as Fig. 3, but for the case  $\hat{c} \parallel \hat{z}$ .FIG. 7. The same as Fig. 3, but for the case  $\hat{c} \parallel \hat{x}$ .

throughout this paper. The experimental spectra for  $K=0.407$  and  $1.175$  are plotted in Figs. 4, 6, and 8. An additional spectrum for  $K=0.530$  is plotted in Fig. 6. For  $K=0.407$  and  $0.530$ , the spectra were recorded, respectively, at  $\theta=24^\circ$  and  $32^\circ$ , and the outside medium was vacuum. For  $K=1.175$ , the spectrum was recorded with the crystal in direct contact with the base of the KRS-5 prism at  $\theta=30^\circ$ . The closed circles shown in the spectra are the inflection points on the smooth edges of the high-reflectivity bands, and they correspond to the closed circles shown in Figs. 3, 5, and 7.

With the aid of Figs. 3, 5, and 7, one can readily assign the frequencies of the inflection points as due to TO, LO, or polariton modes. Only the analysis of the case  $\hat{c} \parallel \hat{y}$  will be given here, since the cases  $\hat{c} \parallel \hat{z}$  and  $\hat{c} \parallel \hat{x}$  can be analyzed in the same way. From Figs. 3 and 4, it is seen that the

frequencies for the first, third, and fifth inflection points from the right correspond to the  $\omega_{T,2}^\perp$ ,  $\omega_{T,3}^\perp$ , and  $\omega_{T,4}^\perp$  mode frequencies, respectively. This is a consequence of the condition (5a),  $\epsilon_\perp \leq 0$ , and the fact that these frequencies are independent of the value of the wave vector. The frequencies for the second, fourth, and sixth inflection points correspond to the polariton mode frequencies. These frequencies depend on the values of the wave vector, because the condition (5b) is satisfied for  $\epsilon_\perp > 0$  and  $k_B^2 - k_x^2 = 0$ . The agreement between the theory and the experiment is good. However, some disagreements did occur. For  $\hat{c} \parallel \hat{z}$  (see Figs. 5 and 6), a sharp peak near  $512 \text{ cm}^{-1}$  is predicted by the theory and is indeed observed experimentally. However, this peak is not reproduced well from Eq. (1) (damping included). The calculated reflectivity spectra appeared as a shoulder instead of a sharp peak near  $512 \text{ cm}^{-1}$ . For  $\hat{c} \parallel \hat{x}$  (see Figs. 7 and 8), a dip near  $625 \text{ cm}^{-1}$  and a peak near  $900 \text{ cm}^{-1}$  are predicted by the theory. However, the experimental results showed that the dip and the peak were observed for large values of  $K$ , but only a weak absorption near  $625 \text{ cm}^{-1}$  and a shoulder near  $900 \text{ cm}^{-1}$  were ob-

FIG. 6. The same as Fig. 4, but for the case  $\hat{c} \parallel \hat{z}$ .FIG. 8. The same as Fig. 4, but for the case  $\hat{c} \parallel \hat{x}$ .

served for small values of  $K$ . The reflectivity spectra calculated from Eq. (1) showed a dip near  $625 \text{ cm}^{-1}$  for large values of  $K$  only but no dip at all at this frequency for small values of  $K$ .

In the above analysis the bulk polariton dispersion curves were calculated from Eq. (4) with damping neglected. However, the dispersion curves can also be obtained from a response function  $T$  proposed by Barker and Loudon:<sup>7</sup>

$$T = \left( k_x - \frac{\omega}{c} \sqrt{\epsilon_z} \right)^{-1}. \quad (7)$$

The dielectric function  $\epsilon_z$  in the above equation has the complete complex form, and the bulk polariton dispersion curves are determined from the calculations of the maxima of  $\text{Im}(T)$  at various values of the wave vector. We calculated the dispersion curves from Eq. (7), and the results

were identical to those calculated from Eq. (4) with zero damping. However, a few additional weak maxima which are not due to bulk polaritons and were not observed in the spectra appeared in the response function calculations. This discrepancy also exists in the calculations for  $\alpha$ -quartz.<sup>2</sup>

#### ACKNOWLEDGMENTS

The authors would like to thank T. L. Ferrell, S. H. Liu, D. L. Mills, and K. R. Subbaswamy for their helpful discussions. The authors also acknowledge partial support of this work from the Oak Ridge National Laboratory's Exploratory Studies Program. This research was sponsored by the Division of Materials Science, U.S. Department of Energy, under Contract No. DE-AC05-84OR21400 with Martin Marietta Energy Systems, Inc.

<sup>1</sup>C. H. Henry and J. J. Hopfield, *Phys. Rev. Lett.* **15**, 964 (1965).

<sup>2</sup>H. J. Falge, A. Otto, and W. Sohler, *Phys. Status Solidi (b)* **63**, 259 (1974).

<sup>3</sup>W. Nitsch, H. J. Falge, and R. Claus, *Z. Naturforsch. Teil A* **29**, 1011 (1974).

<sup>4</sup>L. Merten, *Z. Naturforsch. Teil A* **22**, 359 (1967); **23**, 1183 (1968).

<sup>5</sup>J. Onstott and G. Lucovsky, *J. Phys. Chem. Solids* **31**, 2171 (1970).

<sup>6</sup>D. J. Olechna, *J. Phys. Chem. Solids* **31**, 2755 (1970).

<sup>7</sup>A. S. Barker, Jr. and R. Loudon, *Rev. Mod. Phys.* **44**, 18 (1972).

<sup>8</sup>L. P. Mosteller, Jr. and F. Wooten, *J. Opt. Soc. Am.* **58**, 511 (1968).

<sup>9</sup>W. Sohler, *Opt. Commun.* **10**, 203 (1974).

<sup>10</sup>A. S. Barker, Jr., *Phys. Rev.* **132**, 1474 (1963).